Astron. Astrophys. 339, 286–297 (1998)

ASTRONOMY AND ASTROPHYSICS

Hydrogen line formation in dense magnetized plasmas

S. Brillant[1,2], **G. Mathys**[1], **and C. Stehlé**[2]

[1] European Southern Observatory, Casilla 19001, Santiago 19, Chili
[2] DARC et UPR 176 du CNRS, Observatoire Paris, 5 Place Jules Janssen, F-92190 Meudon, France

Received 9 January 1998 / Accepted 20 July 1998

Abstract. The formation of hydrogen lines in dense plasmas in the presence of a uniform magnetic field is studied. The theory is developed for physical conditions (temperature, electronic density, magnetic field) characteristic of those encountered in the atmospheres of magnetic Ap and Bp stars. This is the first treatment of this problem dealing simultaneously with the Stark effect due to the electric microfields generated by the plasma ions and electrons, the Zeeman effect induced by the magnetic field, and the Stark effect that arises from the Lorentz electric field that the radiating atom is seeing as a result of its motion in the magnetic field. The contribution of the ions is calculated taking into account their dynamics. The Lorentz field introduces a coupling between the intrinsic line broadening and the Doppler effect due to the thermal motion, which in principle severely increases the complexity of the calculations. Special attention is paid to this aspect, and to the discussion of the conditions under which a simplified numerical treatment can be applied.

Key words: line: formation – line: profiles – plasmas – magnetic fields – radiative transfer – polarization

1. Introduction

About 10% of the main-sequence stars with spectral types between F0 and B2 ($7\,10^3$ K $\leq T_{\rm eff} \leq 2.5\,10^4$ K) have very intense magnetic fields (up to a few 10^4 G). These magnetic fields are thought to play a key rôle in the development of strong chemical abundance anomalies in the atmospheres of those chemically peculiar A and B stars (Ap and Bp stars). The interest of those stars lies in the fact that they appear to be the objects showing the most extreme manifestations of physical processes affecting to various extents all the A and B stars close to the main sequence. In their study, the hydrogen lines, especially the Balmer lines, are important diagnostics of the physical conditions prevailing in the atmospheres. Observations of the profiles of those lines in unpolarized light are often used to determine the effective temperature and the surface gravity (e.g., North & Kroll 1989). Their study in circular polarization is a powerful method of determination of the mean longitudinal magnetic field (Landstreet 1982). In particular, this is the only method successfully applied so far to fast rotating stars (Landstreet et al. 1975).

Nevertheless, a proper interpretation of the observations must rely on a correct description of the formation of hydrogen lines in the conditions encountered in the stellar atmospheres under consideration. The aim of the present paper is to present such a description.

The effect of a magnetic field on Stark broadened hydrogen lines has been studied for several decades (Nguyen-Hoe et al. 1966, 1967; Nguyen-Hoe & Drawin 1973). The calculations in those references were based on the assumption that the plasma ions, interacting with the bound electron of the hydrogen atom, could be regarded as fixed in space (static ion approximation). They differed by the treatment of the effect of the plasma electrons on the line shapes. More recently, Mathys (1983, 1984a) performed similar calculations, taking into account the interactions of the fields with the lower levels of the transitions.

Nguyen-Hoe et al. (1981) mentioned the rôle played by the Lorentz electric field ($\boldsymbol{v} \times \boldsymbol{B}/c$) in the unpolarized line profiles of hydrogenic ions moving with a velocity $\boldsymbol{v}$ in a magnetic field $\boldsymbol{B}$. In the meanwhile, it had been demonstrated (Brissaud & Frisch 1971; Kelleher & Wiese 1973) that approaches based on the static ion approximation are inadequate for the description of the H line cores in low and moderate density plasmas. Hence, ion dynamics effects must be taken into account. They yield larger line widths, for lines like Lyα and Hα, and less pronounced dips for Lyβ and Hβ. Line wings are not affected by the ion dynamics effects. Ion dynamics effects in the presence of a magnetic field have been considered by Mathys (1984b), however neglecting the Lorentz electric field.

A formal treatment of the general problem of the polarization of the lines of hydrogen has been presented by Mathys (1985, 1990). As pointed out by this author, the effects of the Lorentz motional field must be studied carefully. While each of the above-mentioned effects (ion motions, Lorentz field contribution, line polarization) has been studied separately, no calculation has been performed up to now including all of them simultaneously.

A less generic case for which parts of the present study may also bear some relevance is that of dense magnetized Tokamak plasmas. One major difference with respect to stellar plasmas is

Send offprint requests to: C. Stehlé

that the hydrogen atoms in Tokamak installations are injected in a collimated, nearly monokinetic neutral beam, which ensures the plasma heating and diagnostic, whereas they have an isotropic Maxwellian velocity distribution in stellar plasmas. Accordingly, the study of Stark broadening for Tokamak plasmas (Voslamber 1995; Derevianko & Oks 1997) deals with a situation different from the one considered here, especially with regard to the average over the velocity of the hydrogen atoms, which is one of the main difficulties of the present study.

In this paper, we present the formalism of the transfer of polarized radiation in hydrogen lines in dense plamas, including both the effects of the Lorentz electric field and of the Doppler shift. The Lorentz electric field is shown to break down the axial symmetry of the problem around the magnetic field. The formalism introduces various elementary profiles for the emission or absorption tensors, which are illustrated for the case of Lyα.

2. Transfer equations

The purpose of this study is to provide a realistic description of the formation of hydrogen lines in magnetized atmospheres. To this effect, we develop the formalism of the radiative transfer in the line $n - n'$. n and n' are the principal quantum numbers of the lower and upper levels of the transition, respectively. The hydrogen atom emits or absorbs radiation at angular frequency ω. It moves with the velocity $\boldsymbol{v}$ in the magnetic field $\boldsymbol{B}$, which is supposed to be uniform at small (atomic) scale. As a result, it is submitted to the action of the Lorentz electric field $\boldsymbol{F}_m = \boldsymbol{v} \times \boldsymbol{B}/c$. Because of the external fields $\boldsymbol{B}$ and $\boldsymbol{F}_m$, the radiation of the hydrogen atom is polarized. Thus, the radiative transfer must be described by a vectorial equation for the Stokes vector $\mathsf{S} = (I, Q, U, V)^t$.

2.1. Definitions

We assume that the radiation, of angular frequency ω, propagates through a plane-parallel atmosphere along the direction $\boldsymbol{k}$, which makes an angle Θ with the normal to the atmosphere (direction Z). Two mutually orthogonal polarization unit vectors $\boldsymbol{e}_1$ and $\boldsymbol{e}_2$ are defined in the plane perpendicular to $\boldsymbol{k}$. In this stellar frame, the transfer equation for the Stokes vector is given by

$$cos\Theta \, \frac{d\mathsf{S}}{dZ} = \chi \, \mathsf{S} - \eta \, , \tag{1}$$

where χ and η are the opacity matrix and emissivity vector defined as

$$\chi = N \, \mathsf{B}_{\mathsf{abs}} - N' \, \mathsf{B}_{\mathsf{em}} \, ; \tag{2}$$

$$\eta = N' \, \frac{2 \, \hbar \, \omega^3}{(2 \, \pi \, c)^2} \, \mathsf{B}_{\mathsf{em}} (1, 0, 0, 0)^t \, . \tag{3}$$

In these expressions, N and N' are the respective populations (per unit of volume) of levels n and n'. $\mathsf{B}_{\mathsf{abs}}$ and B_{em} are the 4×4 absorption and stimulated emission matrices defined by

$$\mathsf{B}_{\mathsf{abs(em)}} = \frac{2 \, \pi^2 \, \omega}{\hbar \, c} \, \mathsf{b}_{\mathsf{abs(em)}} \tag{4}$$

where

$$\mathsf{b}_{\mathsf{abs(em)}} = \begin{pmatrix} \eta_I & \eta_Q & \eta_U & \eta_V \\ \eta_Q & \eta_I & \rho_V & -\rho_U \\ \eta_U & -\rho_V & \eta_I & \rho_Q \\ \eta_V & \rho_U & -\rho_Q & \eta_I \end{pmatrix} , \tag{5}$$

with

$$\begin{aligned} \eta_I &= I_{11} + I_{22} \, , \\ \eta_Q &= I_{11} - I_{22} \, , \\ \eta_U &= I_{12} + I_{21} \, , \\ \eta_V &= -(R_{12} - R_{21}) \, , \\ \rho_Q &= R_{11} - R_{22} \, , \\ \rho_U &= R_{12} + R_{21} \, , \\ \rho_V &= I_{12} - I_{21} \, . \end{aligned} \tag{6}$$

In these expressions, the subscripts 1 and 2 refer to the polarization vectors $\boldsymbol{e}_1$ and $\boldsymbol{e}_2$. I_{kl} is the real part and R_{kl} the imaginary part of the generalized line profile $\mathcal{I}_{kl}(\omega)$ defined by

$$\begin{aligned} \mathcal{I}_{kl}(\omega) &= \sum_{a\alpha, b\beta} r_{aa} <a|D_k|\alpha><\beta|D_l|b> \ll a\alpha|\mathcal{T}(\omega)|b\beta\gg, \\ D_k &= \boldsymbol{e}_k \cdot \boldsymbol{D} \, , \\ D_l &= \boldsymbol{e}_l \cdot \boldsymbol{D} \, . \end{aligned} \tag{7}$$

$\boldsymbol{D}$ is the dipole operator. $\mathcal{T}(\omega)$ is the Fourier transform at ω of the time evolution operator in the Liouville space $\mathcal{T}(t)$, averaged over all the interactions with the plasma and over the velocities of the radiating atom (Appendix A).

Hereafter we denote by greek and roman letters the states corresponding to the lower (n) and upper (n') levels respectively. r_{aa} is the statistical weight of the state a. Except for this factor, the line shapes for emission and absorption are identical. We neglect also, for simplicity, the additive contributions of the absorption and emission backgrounds. For the magnetic field strengths considered in this paper, their polarization may be neglected compared to the line polarization. As the derivations are similar for the absorption and emission matrices, and for the emission vector, we shall restrict the discussion to the case of absorption.

The velocity $\boldsymbol{v}$ of the radiating hydrogen atom is responsible for the usual Doppler shift and for the Lorentz electric field. Thus we shall inspect first the expression of the absorption matrix for a given radiator velocity $\boldsymbol{v}$, which will be denoted by $\mathsf{b}_{\mathsf{abs}}(\omega, \boldsymbol{v}, \theta)$, where θ is the angle between the propagaton vector $\boldsymbol{k}$ and the magnetic field. The absorption matrix of the hydrogen plasma, $\mathsf{b}_{\mathsf{abs}}(\omega, \theta)$, is obtained by averaging $\mathsf{b}_{\mathsf{abs}}(\omega, \boldsymbol{v}, \theta)$ over the velocity distribution of the atoms, $f(\boldsymbol{v})$. Taking into account the Doppler shift $\Delta\omega_D(\boldsymbol{v})$, one obtains:

$$\mathsf{b}_{\mathsf{abs}}(\omega, \theta) = \int d\boldsymbol{v} \, f(\boldsymbol{v}) \, \mathsf{b}_{\mathsf{abs}}(\omega - \Delta\omega_D(\boldsymbol{v}), \boldsymbol{v}, \theta) \, . \tag{8}$$

In the case of negligible Lorentz field, the expression of $\mathsf{b}_{\mathsf{abs}}$ can be obtained in terms of contributions where $\boldsymbol{k}$ is parallel or perpendicular to the magnetic field (Mathys 1985). The inclusion of the Lorentz field breaks the axial symmetry around the

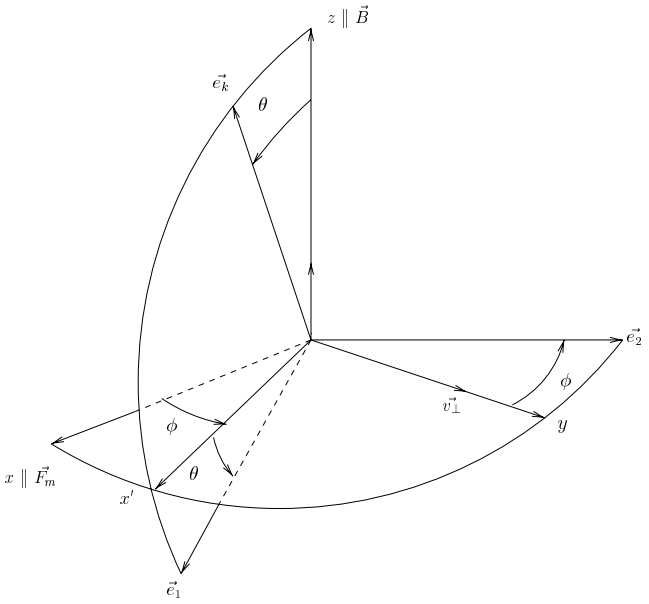

Fig. 1. Geometry of the system

magnetic field and the expression of the above matrices must be studied with respect to the more complicated geometry of the problem.

2.2. Transfer equation in hydrogen lines

Let us define a reference system $Oxyz$ as follows. The z axis is parallel to the magnetic field $\boldsymbol{B}$. The velocity of the hydrogen atom $\boldsymbol{v}$ is in the plane (yOz). Let $v_\parallel$ and $v_\perp$ be its projections along the axis z and perpendicular to it. The Lorentz electric field, $F_m = v_\perp B/c$, is directed along the x axis. The polarization vectors $\boldsymbol{e}_1$ and $\boldsymbol{e}_2$ already introduced are located in the plane perpendicular to $\boldsymbol{k}$. ϕ is the angle between $\boldsymbol{e}_2$ and the y axis (Fig. 1). One has:

$$\begin{aligned} \boldsymbol{e}_1 &= \cos\theta\,\cos\phi\,\boldsymbol{e}_x + \cos\theta\,\sin\phi\,\boldsymbol{e}_y - \sin\theta\,\boldsymbol{e}_z\,, \\ \boldsymbol{e}_2 &= -\sin\phi\,\boldsymbol{e}_x + \cos\phi\,\boldsymbol{e}_{\rm y}\,, \end{aligned} \tag{9}$$

where $\boldsymbol{e}_x$, $\boldsymbol{e}_y$, and $\boldsymbol{e}_z$ are unit vectors along the three axes.

Due to the Doppler shift, the frequency seen by the atom is $\omega - \Delta\omega_D(\boldsymbol{v})$, with

$$\Delta\omega_D(\boldsymbol{v}) = -\frac{\omega_0}{c}\,(v_\parallel\,\cos\theta + v_\perp\,\sin\theta\,\sin\phi)\,. \tag{10}$$

As we are interested in the transfer within a line centered around ω_0, we replaced in the previous equation ω by ω_0.

Doppler shift and Lorentz field are correlated, except in the case where the radiation propagates along the direction of the magnetic field ($\theta = 0$). Thus in the general case, the contribution of the Doppler effect cannot be dealt with by the standard convolution between the natural and Doppler profiles.

Let us express the various dipolar contributions $D_1\,D_1 + D_2\,D_2$, $D_1\,D_1 - D_2\,D_2$, $D_1\,D_2 + D_2\,D_1$, and $D_1\,D_2 - D_2\,D_1$, entering the expression of the elements of the absorption and emission matrices defined in Eqs. (6) and (7). As the Doppler shift depends on $\sin\phi$, the generalized profile is invariant by reflexion about the plane defined by $\boldsymbol{B}$ and $\boldsymbol{k}$ (i.e., if ϕ is replaced by $\pi - \phi$), and terms which are proportional to $\cos\phi$ disappear after average over ϕ. Keeping this in mind , one obtains

$$\begin{aligned} D_1\,D_1 + D_2\,D_2 &= \frac{1}{2}\,(\cos^2\theta + 1)\,(D_x\,D_x + D_y\,D_y) \\ &+ \sin^2\theta\,D_z\,D_z \\ &- \frac{1}{2}\,\sin^2\theta\,\cos 2\phi\,(D_x\,D_x - D_y\,D_y) \\ &- \frac{1}{2}\,\sin 2\theta\,\sin\phi\,(D_y\,D_z + D_z\,D_y)\,, \\ D_1\,D_1 - D_2\,D_2 &= \sin^2\theta\,(D_z\,D_z - \frac{1}{2}\,(D_x\,D_x + D_y\,D_y)) \\ &+ \frac{1}{2}\,(\cos^2\theta + 1)\,\cos 2\phi\,(D_x\,D_x - D_y\,D_y) \\ &- \frac{1}{2}\,\sin\phi\,\sin 2\theta\,(D_y\,D_z + D_z\,D_y)\,, \\ D_1\,D_2 + D_2\,D_1 &= \cos\theta\,\cos 2\phi\,(D_x\,D_y + D_y\,D_x) \\ &+ \sin\theta\,\sin\phi\,(D_x\,D_z + D_z\,D_x)\,, \\ D_1\,D_2 - D_2\,D_1 &= \cos\theta\,(D_x\,D_y - D_y\,D_x) \\ &+ \sin\theta\,\sin\phi\,(D_z\,D_x - D_x\,D_z)\,. \end{aligned} \tag{11}$$

We may write these expressions as a function of the irreducible tensor expression of the dipole operator d^1_q ($q = -1, 0, 1$), using the relations given in Appendix B.

It is easy to see that the absorption matrix $\mathsf{b}(\omega, \boldsymbol{v})$ differs from the one, simpler, which had been obtained by Mathys (1985) neglecting the Lorentz field. The latter will be denoted by $\mathsf{b}_0(\omega, \boldsymbol{v})$. Its elements are:

$$\begin{aligned} \eta_{I,0} &= (\cos^2\theta + 1)\,(I_{xx} + I_{yy})/2 + \sin^2\theta\,I_{zz}\,, \\ \eta_{Q,0} &= \sin^2\theta\,(I_{zz} - (I_{xx} + I_{yy})/2)\,, \\ \eta_{U,0} &= 0\,, \\ \eta_{V,0} &= -\cos\theta\,(R_{xy} - R_{yx})\,, \\ \rho_{Q,0} &= \sin^2\theta\,(R_{zz} - (R_{xx} + R_{yy})/2)\,, \\ \rho_{U,0} &= 0\,, \\ \rho_{V,0} &= \cos\theta\,(I_{xy} - I_{yx})\,. \end{aligned} \tag{12}$$

The difference between b and b_0 is due to the correlation between the Doppler shift (in $v_\perp\,\sin\phi$) and the Lorentz effect $F_m = v_\perp\,B/c$ in the Hamiltonian. The two tensors b and b_0 are equal

1. in the case of axial symmetry about the direction z of the magnetic field. Then the quantum number m is a "good" quantum number. The terms in $D_xD_x - D_yD_y$, $D_xD_y + D_yD_x$, $D_yD_z + D_zD_y$, and $D_xD_z - D_zD_x$ disappear, as a consequence of the selection rule on $\Delta m = m_\alpha - m_a$ (see Appendix C.1). This happens when the Lorentz field is neglected or has no incidence on the line shape (isolated lines).
2. after average over ϕ, when the generalized profile $I + iR$ is independent of ϕ. This happens when the Doppler shift is negligible.

Moreover, the expression of b may be simplified if $\mathcal{T}$ is symmetrical about its diagonal (i.e., $\ll a\alpha|\mathcal{T}(\omega)|b\beta\gg = \ll b\beta|\mathcal{T}(\omega)|a\alpha\gg$). This last property is true for the lines of hydrogen perturbed by the plasma (Stark broadening), in magnetic and Lorentz electric fields. In this case, using the relation $<lm|d^1_q|l'm'> = -<l'm'|d^1_{-q}|lm>^*$, one shows that the terms in $D_x\,D_y + D_y\,D_x$, $D_y\,D_z + D_z\,D_y$, and $D_x\,D_z - D_z\,D_x$, cancel out after summation over the states $a\alpha, b\beta$ mentioned in Eq. (7) (Appendix C.2).

Thus the absorption matrix can be decomposed in two contributions:

$$\mathsf{b} = \mathsf{b}_0 + \cos 2\phi\, \mathsf{b}_{\mathsf{cross}}\,. \tag{13}$$

The first, $\mathsf{b}_0(\omega, \boldsymbol{v})$, is given above. The second one, proportional to $\cos 2\phi$, is due to the correlation between the Doppler shift and the Lorentz effect in the Hamiltonian. It will be denoted by $\mathsf{b}_{\mathsf{cross}}(\boldsymbol{v})$. Its elements are:

$$\begin{aligned}
\eta_{I,cross}/\cos 2\phi &= -\sin^2\theta\,(I_{xx} - I_{yy})/2\,,\\
\eta_{Q,cross}/\cos 2\phi &= (\cos^2\theta + 1)\,(I_{xx} - I_{yy})/2\,,\\
\eta_{U,cross}/\cos 2\phi &= 0\,,\\
\eta_{V,cross}/\cos 2\phi &= 0\,,\\
\rho_{Q,cross}/\cos 2\phi &= (\cos^2\theta + 1)\,(R_{xx} - R_{yy})/2\,,\\
\rho_{U,cross}/\cos 2\phi &= 0\,,\\
\rho_{V,cross}/\cos 2\phi &= 0\,.
\end{aligned} \tag{14}$$

It is easy to verify that $\mathsf{b}_{\mathsf{cross}}$ vanishes after average over the frequency (Appendix C.3).

2.3. Average over the hydrogen velocity

The absorption matrix $\mathsf{b}(\omega, \theta)$ is obtained after average of the elementary absorption matrix $\mathsf{b}(\omega - \Delta\omega_D(\boldsymbol{v}), \theta, v_\perp, \phi)$ over the velocities of the moving hydrogen atoms. The probability of having the velocity between $\boldsymbol{v}$ and $\boldsymbol{v} + d\boldsymbol{v}$ is:

$$f(\boldsymbol{v})\,d\boldsymbol{v} = d\phi\, v_\perp\, dv_\perp\, dv_\parallel\, f_\perp(v_\perp)\, f_\parallel(v_\parallel)\,. \tag{15}$$

Beside the Doppler shifted frequency $(\omega - \Delta\omega_D(\boldsymbol{v}))$, the dependence of b on the perpendicular velocity $v_\perp$ is a consequence of the interaction of the atom with the Lorentz electric field. The dependences on θ and on ϕ come from the multiplicative factors ($\sin^2\theta$, $\cos^2\theta$, $\cos\theta$, and $\cos 2\phi$). They will be omitted to simplify the notations: that is, we shall write $\mathsf{b}(\omega, v_\perp)$ for $\mathsf{b}(\omega, \theta, v_\perp, \phi)$.

Introducing $<v> = (2kT/M_H)^{1/2}$ (M_H is the mass of the hydrogen atom and T the plasma temperature), $\omega_D = \omega_0 <v>/c$, and $\tilde{\omega} = \omega/\omega_D$, one obtains

$$\begin{aligned}
&\mathsf{b}(\omega, \theta)\\
&= \frac{1}{\pi\sqrt{\pi}<v>^3}\int_0^\infty dv_\perp \exp\left(-\frac{v_\perp^2}{<v>^2}\right) v_\perp\\
&\times \int_{-\infty}^{+\infty} dv_\parallel \exp\left(-\frac{v_\parallel^2}{<v>^2}\right)\\
&\times \int_{-\pi}^{+\pi} d\phi\, \mathsf{b}\left(\omega - \frac{\omega_0}{c}\,(v_\parallel\cos\theta + v_\perp \sin\theta\,\sin\phi), v_\perp\right);
\end{aligned} \tag{16}$$

$$\begin{aligned}
&\mathsf{b}(\tilde{\omega}, \theta)\\
&= \frac{1}{\pi\sqrt{\pi}\cos\theta\sin^2\theta}\int_0^\infty du_\perp \exp\left(-\frac{u_\perp^2}{\sin^2\theta}\right) u_\perp\\
&\times \int_{-\infty}^{+\infty} du_\parallel \exp\left(-\frac{u_\parallel^2}{\cos^2\theta}\right) \int_{-\pi}^{+\pi} d\phi\, \mathsf{b}\,(\tilde{\omega}', u_\perp)\,,
\end{aligned} \tag{17}$$

where $\tilde{\omega}' = \tilde{\omega} - u_\parallel - u_\perp \sin\phi$, with $u_\parallel = v_\parallel \cos\theta/<v>$ and $u_\perp = v_\perp \sin\theta/<v>$.

This expression can also be written also under the form of a convolution product:

$$\mathsf{b}(\tilde{\omega}, \theta) = (g_{\parallel,\theta} * \mathsf{b}_{\perp,\theta})\,(\tilde{\omega})\,, \tag{18}$$

with

$$\begin{aligned}
g_{\parallel,\theta}(\tilde{\omega}) &= \frac{1}{\sqrt{\pi}\,\cos\theta}\exp\left(-\frac{\tilde{\omega}^2}{\cos^2\theta}\right),\\
\mathsf{b}_{\perp,\theta}(\tilde{\omega}) &= \frac{1}{\pi\,\sin^2\theta}\int_0^\infty du_\perp\, u_\perp \exp\left(-\frac{u_\perp^2}{\sin^2\theta}\right)\\
&\quad\times \int_{-\pi}^{+\pi} d\phi\, \mathsf{b}\,(\tilde{\omega} - u_\perp\,\sin\phi, u_\perp)\,.
\end{aligned} \tag{19}$$

In general the average over the velocity $\boldsymbol{v}$ requires three integrations (Eq. 17). This procedure may be simplified in the following cases:

1. If the elementary tensor b depends only negligibly on $u_\perp$ (i.e., $\mathsf{b}(\tilde{\omega}, u_\perp) \simeq \mathsf{b}(\tilde{\omega}, 0)$). Then,

$$\begin{aligned}
\mathsf{b}_{0\perp,\theta}(\tilde{\omega}) &= g_{x,\theta} * \mathsf{b}_0(\tilde{\omega})\,,\\
\mathsf{b}_{\mathsf{cross}\perp,\theta}(\tilde{\omega}) &= 0\,,
\end{aligned} \tag{20}$$

with

$$g_{x,\theta} = \frac{1}{\sqrt{\pi}\,\sin\theta}\int_{-\infty}^{+\infty} du'_x \exp\left(-\frac{u'_x}{\sin^2\theta}\right). \tag{21}$$

In this expression, u'_x is the projection of $\boldsymbol{v}/<v>$ on the axis which corresponds to the intersection of the plane $(\boldsymbol{B}, \boldsymbol{k})$ with the plane perpendicular to $\boldsymbol{B}$. In this case, one recovers the usual standard expression for the averaged absorption tensor,

$$\mathsf{b}_0(\tilde{\omega}, \theta) = (g_{\mathrm{Dopp}} * \mathsf{b}_0)(\tilde{\omega})\,, \tag{22}$$

with

$$g_{\mathrm{Dopp}}(\tilde{\omega}) = \frac{1}{\sqrt{\pi}}\exp(-\tilde{\omega}^2) = g_{\parallel,\theta} * g_{x,\theta}(\tilde{\omega})\,. \tag{23}$$

2. When the quadratic perturbation theory is valid for the interaction with the Lorentz electric field, the elementary absorption tensors for a given velocity may be developed as

$$\mathsf{b}(\tilde{\omega}', u_\perp) = \mathsf{b}^{(0)}(\tilde{\omega}') + u_\perp^2\,\mathsf{b}^{(2)}(\tilde{\omega}')\,. \tag{24}$$

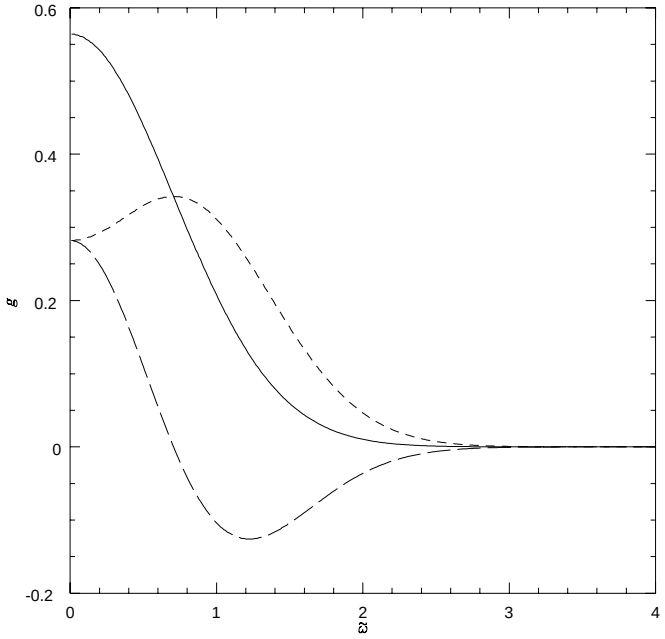

Fig. 2. Variations of g_0 (*short dashes*), g_{cross} (*long dashes*), and $g_{\rm Dopp}$ (*full line*) with $\tilde{\omega}$

Averaging $\mathsf{b}^{(0)}$ over the velocity is straightforward (Eqs. (22) and (23)). Due to the term in $\cos 2\phi$, the averages of the remaining contribution $u_\perp^2\,\mathsf{b}^{(2)}$ differ for b_0 and $\mathsf{b}_{\rm cross}$. One obtains (Appendix D)

$$\mathsf{b}_{0(\rm cross)}(\tilde{\omega},\theta) \;=\; g_{\rm Dopp} * \mathsf{b}^{(0)}_{0(\rm cross)}(\tilde{\omega}) + g_{0(cross)} * \mathsf{b}^{(2)}_{0(\rm cross)}(\tilde{\omega})\,, \qquad (25)$$

with

$$g_0(\tilde{\omega}) = \frac{\sin^4\theta}{\sqrt{\pi}}\,\left[\left(-\frac{1}{2}+\tilde{\omega}^2\right)+\frac{1}{\sin^2\theta}\right]\,\exp(-\tilde{\omega}^2) \quad (26)$$

and

$$g_{cross}(\tilde{\omega}) = \frac{\sin^4\theta}{\sqrt{\pi}}\,\left[\frac{1}{2}-\tilde{\omega}^2\right]\,\exp(-\tilde{\omega}^2)\,. \qquad (27)$$

Fig. 2 shows the variation of the two functions g_0 and g_{cross} for $\theta = \pi/2$ together with the standard Doppler profile $g_{\rm Dopp}(\tilde{\omega})$.

The last procedure allows one to simplify the velocity average of the absorption matrices. It rests on the assumption that the Lorentz electric field effects can be described within a perturbative approach. In the general case, the three integrations over $u_\parallel$, $u_\perp$, and ϕ (Eq. (17)) cannot be avoided.

3. Application to the hydrogen lines

Let us consider an hydrogen atom moving with the velocity $\boldsymbol{v}$ in a neutral plasma composed of free electrons and protons. The electron density (number of electrons per unit of volume) is N_e; it is equal to the ion density. The charges of the plasma create two electric microfields, one for the electrons ($\boldsymbol{E}_e$) and the other for the ions ($\boldsymbol{E}_i$). The relative importance of the effects of the plasma, the magnetic field (through the Zeeman effect), and its associated Lorentz electric field, already studied by Mathys (1990), is discussed below for plasmas representative of typical stellar atmospheres.

Our primary goal is to check if the approximation of perturbative quadratic treatment of the Lorentz field effects in the lines is physically relevant. Accordingly, while the basic considerations underlying the line shape calculations are presented in detail below, we shall afterwards introduce some simplifications, in order to clarify the discussion. We shall check that the approximations made do not alter the conclusions that are drawn.

3.1. Elementary interactions

The Holtsmark mean field F_0 gives the order of magnitude of the mean electric microfield of the plasma. Its value is given by

$$F_0 \;=\; e^2\,\left(\frac{4\pi}{3}\right)^{2/3}\,N_e^{2/3} \;=\; 1.25\,10^{-9}\,N_e^{2/3} \quad (\mathrm{cm}^{-3},\ \mathrm{ues})\,. \qquad (28)$$

For an atom moving with the thermal velocity $<v>$, the Lorentz electric field is

$$F_m = <v_\perp> B/c = 4.28\,10^{-7}\,T^{1/2}\,B \quad (\mathrm{G},\ \mathrm{K},\ \mathrm{ues})\,. \qquad (29)$$

The Holtsmark and Lorentz fields are equal for magnetic fields B such that

$$B = 2.92\,10^{-3}\,N_e^{2/3}\,T^{-1/2} \quad (\mathrm{G},\ \mathrm{K},\ \mathrm{cm}^{-3})\,. \qquad (30)$$

The hamiltonian describing the internal state of the hydrogen atom in the geometry of the system under consideration is

$$H \;=\; H_0 + H_s + H_Z + H_m\,,$$

with

$$\begin{aligned} H_s &= -\boldsymbol{D}\cdot(\boldsymbol{E}_e+\boldsymbol{E}_i)\,,\\ H_Z &= \hbar\,\omega_L\,L_z\,,\\ H_m &= -D_x\,F_m\,. \end{aligned} \qquad (31)$$

In those expressions, $\omega_L = e\,B/(2m_e\,c)$ is the Larmor frequency, and L_z is the z component of the (orbital) atomic angular momentum. H_0 is the hamiltonian of the isolated atom, H_s is the hamiltonian of its dipolar interaction with the random electric plasma microfields, H_Z is the Zeeman hamiltonian, and H_m is the hamiltonian of interaction with the Lorentz electric field.

In the expression of H_Z, we take into account only the contribution of the orbital angular momentum of the electron, and we neglect the spin, hence the fine structure. This approximation is supported by the following arguments. The present work is a first step in the study of a complex physical problem, and its primary purpose is to establish the foundations of the methodology that will be used later on in this study. Consequently,

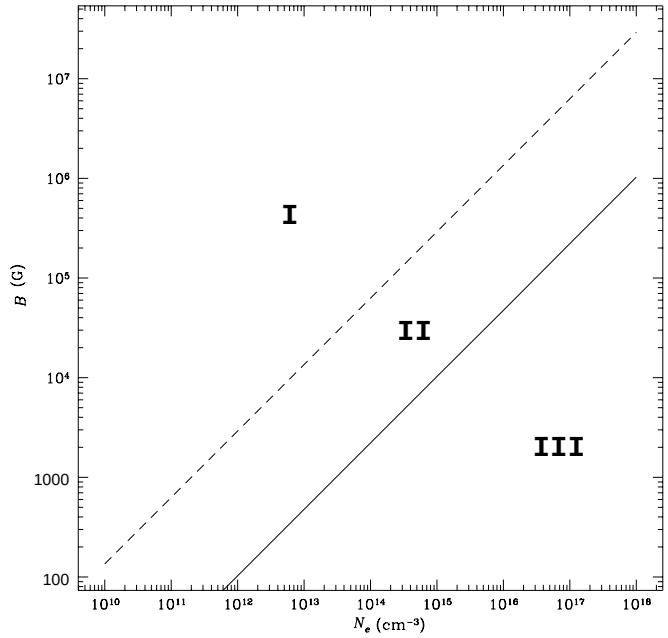

Fig. 3. Loci of equal Zeeman and plasma Stark effects (*solid line*) and of equal motional and plasma Stark effect (*dashes*), for a temperature of 10^4 K and for a principal quantum number n equal to 2

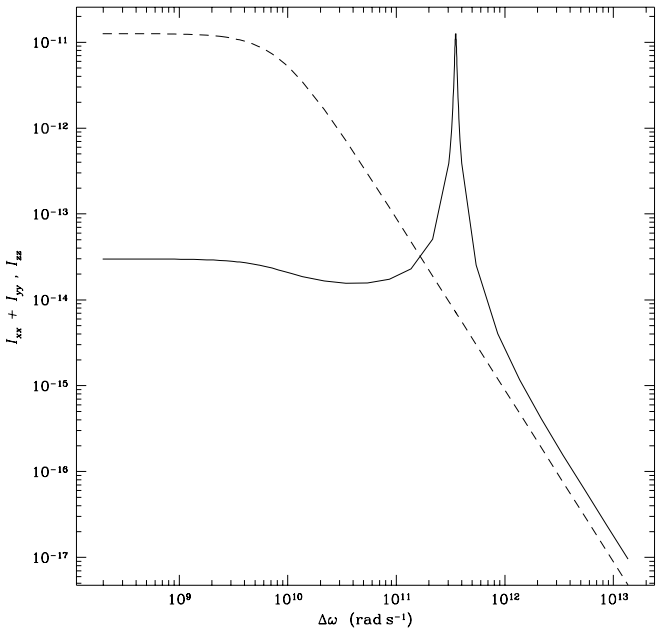

Fig. 4. Variation with the detuning $\Delta\omega$ of the functions $(I_{xx} + I_{yy})$ (*solid line*) and I_{zz} (*dashed line*) for the Lyα transition, in the following conditions: temperature: 10^4 K; density: $N_e = 10^{14}$ cm^{-3}; magnetic field: 40 kG; $u_\perp = 1$; and $\gamma(\Delta\omega)$ constant, equal to $\gamma(0)$. Only the part of the functions for which $\Delta\omega > 0$ is represented: both profiles are symmetrical about the line centre

at this stage, the emphasis is not on deriving theoretical profiles that are realistic in every detail, but rather on exploring the respective contributions of the various physical processes involved and the most practical way to deal with them. Within this framework, including the fine structure makes the numerical experiment considerably more intricate without providing significant additional insight into the core of the problem, that is, the combined effect of the magnetic and electric fields on the line profiles. Furthermore, an estimate of the orders of magnitude of the various relevant physical effects indicates that the influence of the fine structure can at most be marginal in practice. Indeed, for the level $n = 2$, the separation of the states $j = 1/2$ and $j = 3/2$ is approximately $7\,10^{10}$ rd s^{-1}. This is to be compared with the Larmor frequency ω_L, characterizing the magnitude of the Zeeman splitting of the level, and with the frequency ω_D corresponding to the half-width at half-maximum of the thermal Doppler profile of Lyα.[1] For the sample case discussed below of $T = 10^4$ K and $B = 40$ kG, these frequencies are, resp., $\omega_D = 5.6\,10^{11}$ rd s^{-1} and $\omega_L = 3.5\,10^{11}$ rd s^{-1}: both are significantly greater than the fine structure.

The relative orders of magnitude of the various shifts: Lorentz $\Delta\omega_m = 1.5\,n\,(n-1)\,e\,a_0\,F_m/\hbar$, Stark $\Delta\omega_s = 1.5\,n\,(n-1)\,e\,a_0\,F_0/\hbar$, and Zeeman $\Delta\omega_L = (n-1)\,\omega_L$, are for level n:

$$\begin{aligned} \Delta\omega_m/\Delta\omega_s &= 342\,T^{1/2}\,B/(n\,N_e^{2/3}) \quad (\mathrm{G},\ \mathrm{K},\ \mathrm{cm}^{-3})\,, \\ \Delta\omega_L/\Delta\omega_m &= 5679/(n\,T^{1/2}) \quad (\mathrm{K})\,. \end{aligned} \tag{32}$$

[1] Even though the profiles illustrated in this paper are not Doppler broadened, in the practical astrophysical situations to which this treatment will be applied in the future, Doppler broadening will always be present.

Fig. 3 illustrates three typical domains of electronic density–magnetic field conditions. In the portion of the plane below the lower line (region III), the effects of both the Lorentz and magnetic fields are negligible. One expects the line polarization to be small and the line shapes to be described within the standard plasma Stark broadening theory. In region II, located between the two lines, the Zeeman splitting will be resolved and the Lorentz field is negligible compared to the plasma normal field value. The line polarization will be larger. In region I (upper part of the figure), the Zeeman splitting is resolved, and the effects of the motional electric field (larger than the normal Holtsmark field) should be noticeable in the absorption tensor.

3.2. Generalized line profile

To obtain the transfer matrix, it is necessary to compute the generalized line profile $\mathcal{I}$, or more precisely the Fourier transform of the evolution operator $\mathcal{T}(t,0)$, which is solution of the Liouville equation

$$i\,\hbar\,\frac{d\mathcal{T}(t,0)}{dt} = \mathcal{L}\,\mathcal{T}(t,0)\,. \tag{33}$$

One of the difficulties is to describe correctly the time fluctuations of the plasma microfields. The two microfields constitute random dynamical processes whose typical time scales differ significantly. These times scales are the inverse of the electronic or ionic plasma frequencies for the electrons and for the ions, $\omega_{p,e(H^+)} = \sqrt{4\,\pi\,e^2\,N_e/m_e(M_H)}$. Except for very dense plasmas or optical transitions involving a Rydberg level ($n \gg 1$),

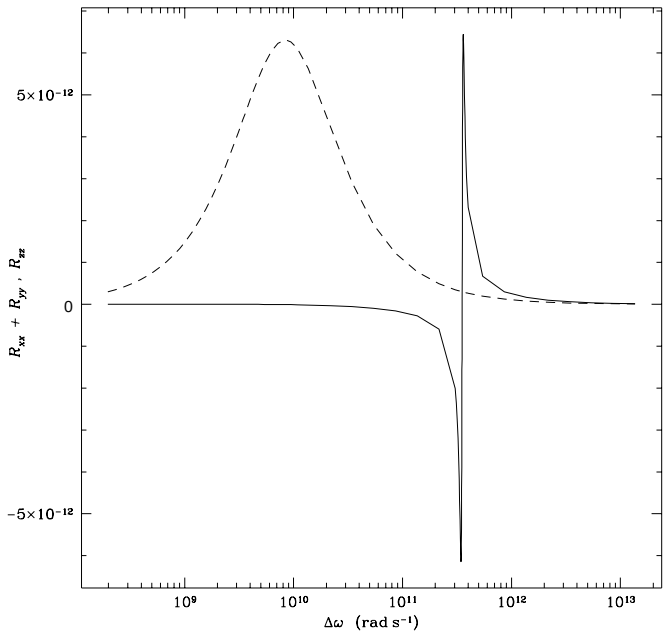

Fig. 5. Variation with $\Delta\omega$ of the functions $(R_{xx}+R_{yy})$ (*solid line*) and R_{zz} (*dashed line*) for the Lyα transition, in the same conditions as in Fig. 4. Both profiles are antisymmetrical about the line centre

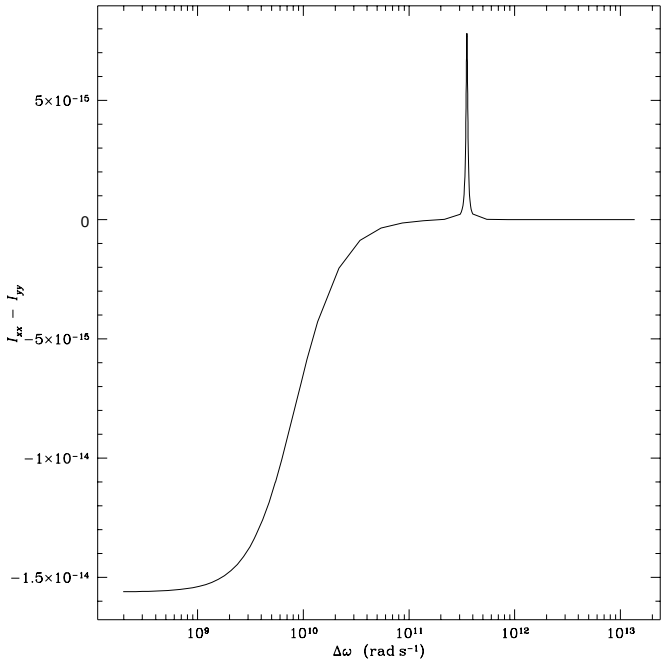

Fig. 6. Variation with $\Delta\omega$ of the function $(I_{xx}-I_{yy})$ for the Lyα transition, in the same conditions as in Fig. 4. This profile is antisymmetrical about the line centre

the contribution of the plasma electrons to the line shape may be described within the Unified Theory, i.e., in terms of the frequency dependent damping rate $\gamma_e(\omega)$ (Vidal et al. 1970). For the ionic contribution to the line, the situation is more complex. At high densities it is reasonable to use the static ion approximation, which supposes that the ions do not have the time to move during the radiative process. However, at low densities (less than 10^{15} cm^{-3} for $T = 10^4$ K, and the line Lyα), the ion dynamics effects are known to be important in the line centers (Stehlé et al. 1983) and the Unified Theory is valid for both the ions and the electrons. Then, introducing for the ions the damping rate $\gamma_i(\omega)$, one has

$$\mathcal{T}(\omega) \;=\; -i\pi^{-1}\,(\mathcal{L} - \omega\, I - i\,\gamma(\omega))^{-1}\,, \tag{34}$$

where

$$\gamma(\omega) \;=\; \gamma_e(\omega) + \gamma_i(\omega)\,. \tag{35}$$

The total relaxation operator $\gamma(\omega)$ is constant in the line center, up to a frequency detuning ($\Delta\omega = \omega - \omega_0$) equal to the plasma frequency. It decreases in the far wings as $|\Delta\omega|^{-1/2}$.

We shall illustrate below the typical behaviour of the various quantities introduced above. We make the approximation that the damping rate γ is independent of the frequency, and in order to simplify the discussion, that it is a scalar (while quite generally, it is a tensor). In this case, it is possible to verify that for a fixed transverse hydrogen velocity $u_\perp$, the relevant generalized line shapes can be expressed as

$$\begin{aligned}
(I_{xx}+I_{yy}) \;+\; i\,(R_{xx}+R_{yy}) &= \frac{i}{6\pi}\,\left(\frac{1}{1+9A^2}\right)\\
\times\Bigg[\frac{18\,A^2}{z+i\,y} \;+\; &\frac{2+9A^2}{z+\sqrt{1+9A^2}+i\,y}\\
+\; &\frac{2+9A^2}{z-\sqrt{1+9A^2}+i\,y}\Bigg]\,,\\
I_{zz}+i\,R_{zz} \;=\; &\frac{i}{3\pi}\left[\frac{1}{z+i\,y}\right]\,,\\
(I_{xx}-I_{yy}) \;+\; i\,(R_{xx}-R_{yy}) &= \frac{-i}{6\pi}\,\left(\frac{9A^2}{1+9A^2}\right)\\
\times\Bigg[\frac{2}{z+i\,y} \;-\; &\frac{1}{z+\sqrt{1+9A^2}+i\,y}\\
-\; &\frac{1}{z-\sqrt{1+9A^2}+i\,y}\Bigg]\,,\\
(I_{xy}-I_{yx}) \;+\; i\,(R_{xy}-R_{yx}) &= \frac{-1}{3\pi}\,\left(\frac{1}{\sqrt{1+9A^2}}\right)\\
\times\Bigg[\frac{1}{z+\sqrt{1+9A^2}+i\,y} \;-\; &\frac{1}{z-\sqrt{1+9A^2}+i\,y}\Bigg]\,.
\end{aligned} \tag{36}$$

In these expressions,

$$\begin{aligned}
A \;&=\; e\,a_0\,F_m/(\hbar\,\omega_L) = 1.17\,10^{-4}\,T^{1/2}\,u_\perp \quad (T \text{ in K}),\\
y \;&=\; \gamma/\omega_L\,,\\
z \;&=\; \Delta\omega/\omega_L\,.
\end{aligned} \tag{37}$$

With the adopted notations, the various quantities I_{kl} and R_{kl} are normalized in z. In other words, one has, e.g., $I_{kl}(z) = \omega_L\, I_{kl}(\omega)$.

The typical variations of these various quantities are illustrated in Figs. 4 to 9, for $T = 10^4$ K, $B = 40$ kG, a scalar damping rate γ corresponding to an electronic density

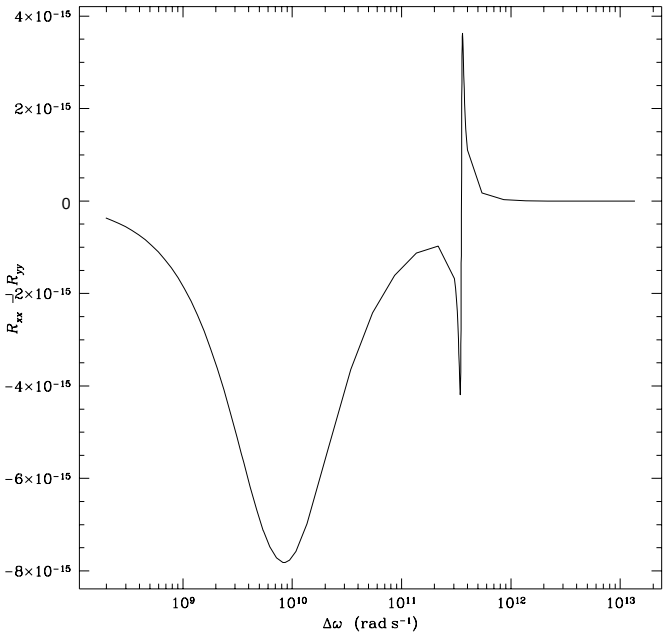

Fig. 7. Variation with $\Delta\omega$ of the function $(R_{xx} - R_{yy})$ for the Lyα transition, in the same conditions as in Fig. 4. This profile is symmetrical about the line centre

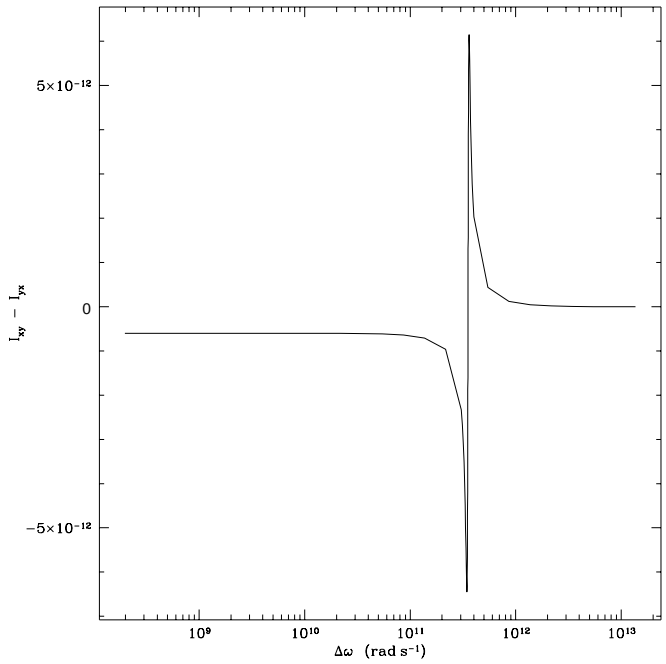

Fig. 8. Variation with $\Delta\omega$ of the function $(I_{xy} - I_{yx})$ for the Lyα transition, in the same conditions as in Fig. 4. This profile is symmetrical about the line centre

$N_e = 10^{14}$ cm^{-3}, and a mean transverse velocity $u_\perp = 1$. In those conditions, $\omega_L = 3.5\,10^{11}$ rad s^{-1}, $A = 1.17\,10^{-2}$, $\Delta\omega_D/\omega_L = 1.59$, and $\gamma/\omega_L = 2.4\,10^{-2}$. Except for the quadratic shift in the position of the resonances, which is negligible compared to their width γ,[2] the various contributions can be developed in powers of A^2 or $u_\perp^2$. Thus, let us introduce the relative variations $\delta(R_{xx} + R_{yy})$, $\delta(I_{xx} + I_{yy})$, $\delta(R_{xx} - R_{yy})$, $\delta(I_{xx} - I_{yy})$, $\delta(I_{xy} - I_{yx})$, and $\delta(R_{xy} - R_{yx})$:

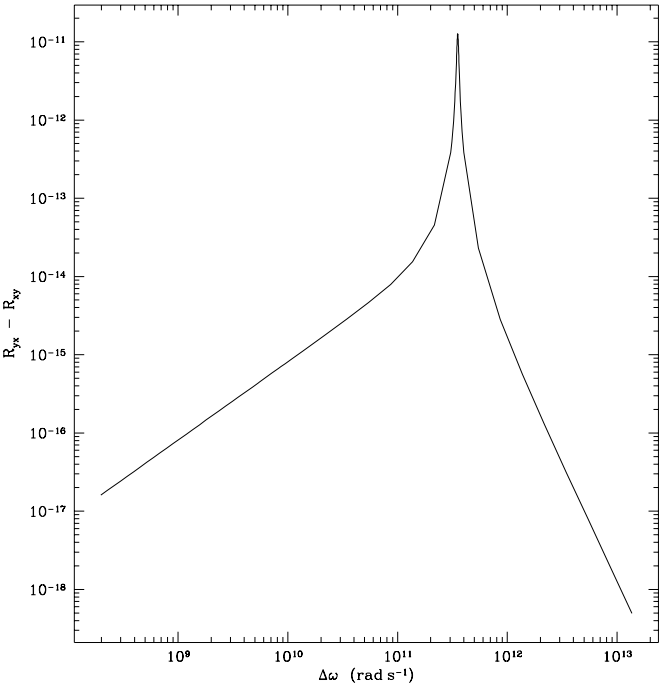

Fig. 9. Variation with $\Delta\omega$ of the function $(R_{yx} - R_{xy})$ for the Lyα transition, in the same conditions as in Fig. 4. This profile is symmetrical about the line centre

$$\delta(R_{xx} + R_{yy}) = \frac{1}{u_\perp^2}\left[(R_{xx} + R_{yy})_{u_\perp} - (R_{xx} + R_{yy})_{u_\perp=0}\right], \quad (38)$$

$$\delta(I_{xx} + I_{yy}) = \frac{1}{u_\perp^2}\left[(I_{xx} + I_{yy})_{u_\perp} - (I_{xx} + I_{yy})_{u_\perp=0}\right], \quad (39)$$

$$\delta(R_{xx} - R_{yy}) = \frac{1}{u_\perp^2}\left[(R_{xx} - R_{yy})_{u_\perp} - (R_{xx} - R_{yy})_{u_\perp=0}\right], \quad (40)$$

$$\delta(I_{xx} - I_{yy}) = \frac{1}{u_\perp^2}\left[(I_{xx} - I_{yy})_{u_\perp} - (I_{xx} - I_{yy})_{u_\perp=0}\right], \quad (41)$$

$$\delta(I_{xy} - I_{yx}) = \frac{1}{u_\perp^2}\left[(I_{xy} - I_{yx})_{u_\perp} - (I_{xy} - I_{yx})_{u_\perp=0}\right], \quad (42)$$

$$\delta(R_{yx} - R_{xy})$$

[2] Since our objective is not the detailed calculation of the profiles, we have deliberately taken the approach of simplifying γ. Hence, the operator $\gamma(\Delta\omega)$ is replaced by the scalar $\gamma_{1s2p,1s2p}$ obtained when the magnetic field effect is neglected, such as given e.g. by Stehlé (1994). The value of γ/ω_L adopted for the illustration of Figs. 4 to 9 corresponds to this approximation.

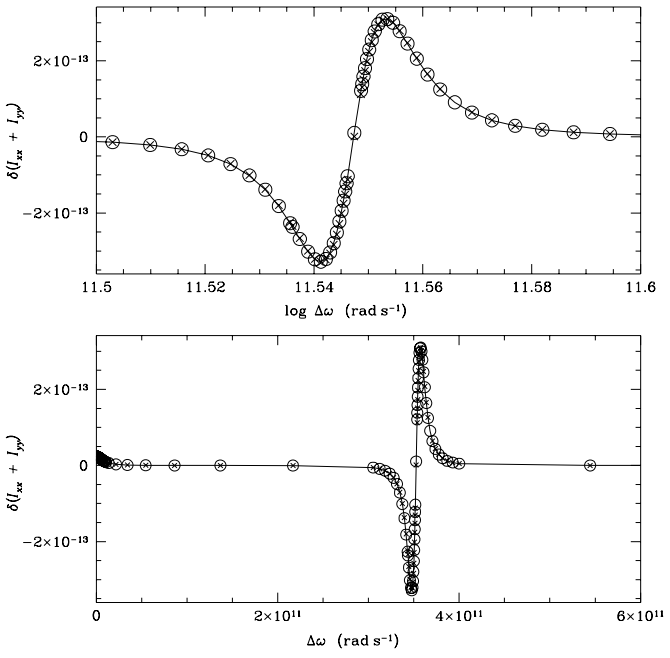

Fig. 10. Variation with $\Delta\omega$ of the function $\delta(I_{xx} + I_{yy})$ for the Lyα transition, in the same plasma conditions (temperature, density, magnetic field) as in Fig. 4. *Solid line*: $u_\perp = 1/3$; *circles*: $u_\perp = 1$; *crosses*: $u_\perp = 2$. This profile is antisymmetrical about the line centre. The top panel is a blown up view of the part of the bottom panel around the Zeeman resonance

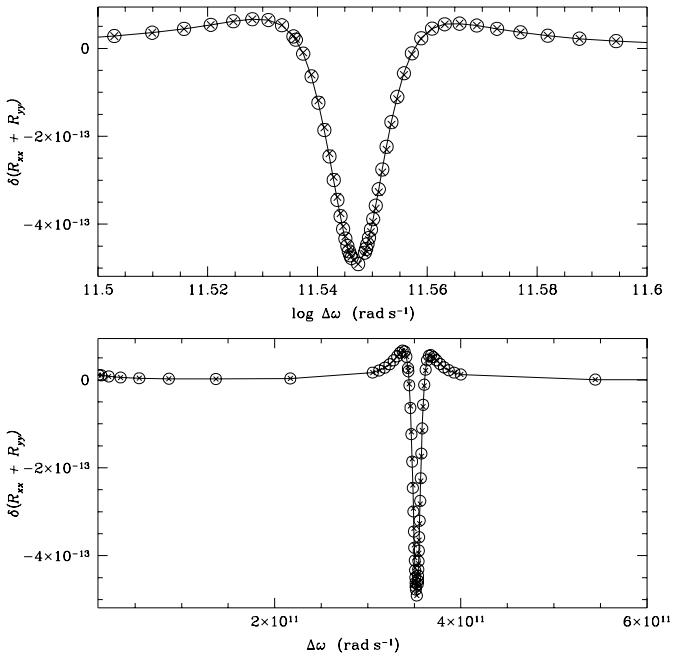

Fig. 11. Same as Fig. 10 for the function $\delta(R_{xx} + R_{yy})$. This profile is symmetrical about the line centre

$$= \frac{1}{u_\perp^2}\left[(R_{yx} - R_{xy})_{u_\perp} - (R_{yx} - R_{xy})_{u_\perp=0}\right] . \qquad (43)$$

The variations of these quantities with the frequency, reported for different values of the velocity in Figs. 10 to 15, indicate that, except in a very small region of the frequency range, close to the Zeeman resonance, they can be considered as independent of the transverse velocity of the hydrogen atom. Thus the method proposed for the calculation of the velocity average in Sect. 2.3 (case 2) is applicable. The incidence of the quadratic shift on the frequency variations is quite negligible as long as the broadening parameter γ is larger than $9A^2$, which is presently the case.

For the line Lyα, the effect of the Lorentz field may be treated perturbatively in comparison with the Zeeman splitting for all temperatures below 10^5 K, for magnetic fields and electronic densities such that

$$\log B \lesssim -3.8 + 0.4 \log N_e \quad (\mathrm{G},\ \mathrm{cm}^{-3}) . \qquad (44)$$

The expansion of b in $u_\perp^2$ is justified as long as the energy perturbation of the Zeeman components induced by the Lorentz field is negligible on scales of the order of γ. This may be questionable at low density and high magnetic field values and should be tested for practical applications.

The results derived in this section remain valid for a more realistic treatment of γ, that is, when γ is not a scalar and depends on the detuning. In this case, the expressions (36) are no longer valid (except in the line wings), and the Liouville operator must be calculated numerically. The impact of the approximations made can be perceived for $I_{xx} + I_{yy}$ (the "usual" unpolarized intensity profile) from the consideration of Fig. 16. In this figure, the static wing limit (for ions and electrons) is overplotted. It is well known that, since dynamical effects decrease in the line wings, the actual profiles should tend towards this static limit away from the line centre. As seen in the figure, this behaviour cannot be reproduced using a frequency independent damping rate.

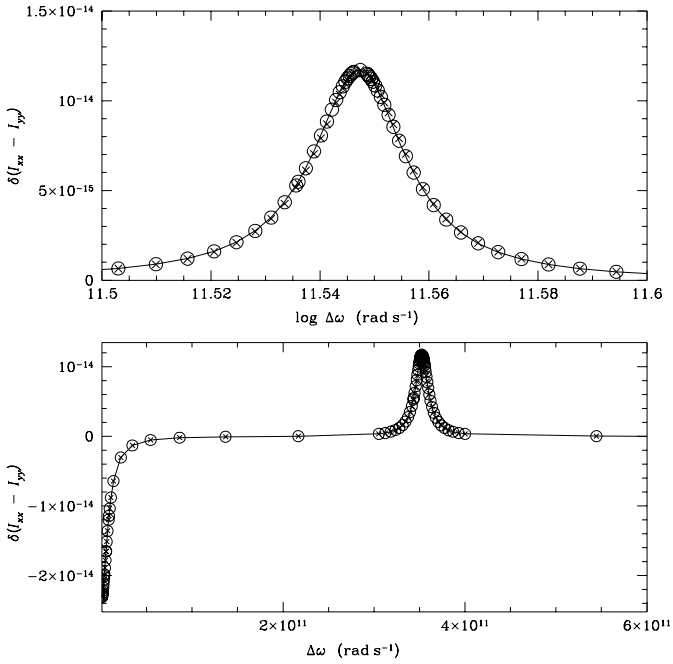

Fig. 12. Same as Fig. 10 for the function $\delta(I_{xx} - I_{yy})$. This profile is symmetrical about the line centre

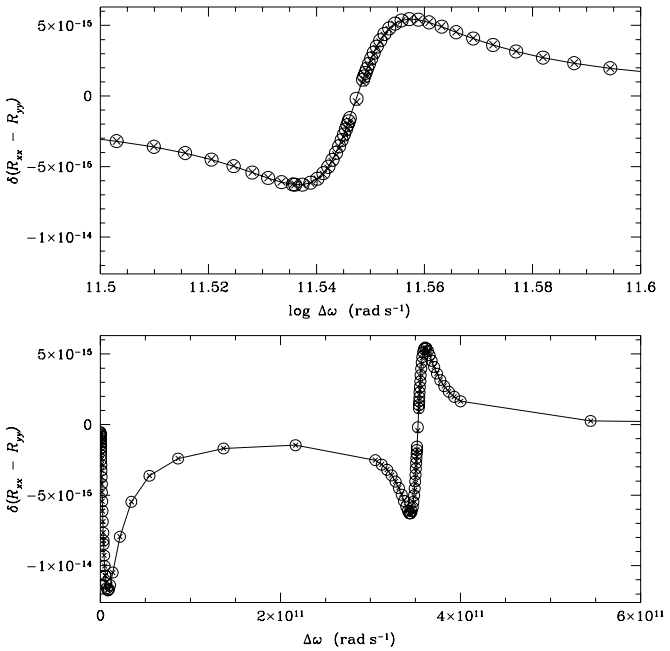

Fig. 13. Same as Fig. 10 for the function $\delta(R_{xx} - R_{yy})$. This profile is antisymmetrical about the line centre

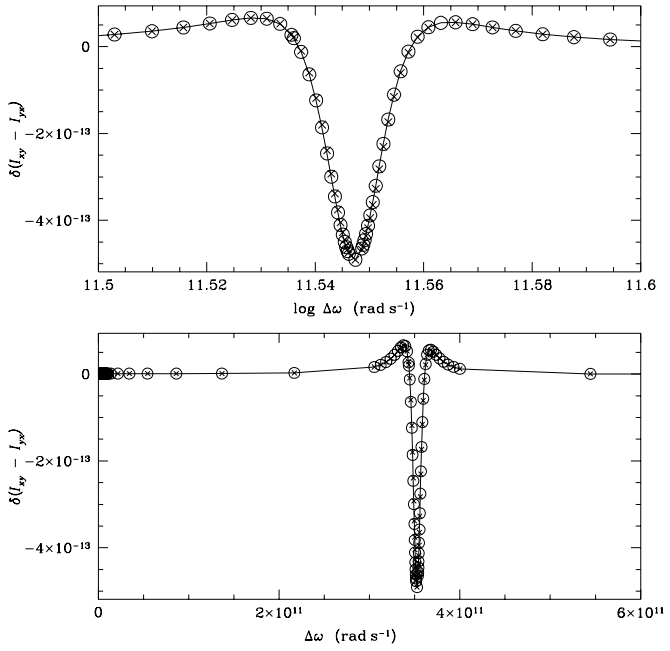

Fig. 14. Same as Fig. 10 for the function $\delta(I_{xy} - I_{yx})$. This profile is symmetrical about the line centre

4. Conclusion

We have investigated the influence of the combined effects of the magnetic and Lorentz electric fields on the expression of the generalized absorption matrix for polarized radiative transfer. We have shown that, for a given velocity of the hydrogen atom, the Lorentz electric field breaks down the axial symmetry of the system about the magnetic field. Because of the correlation

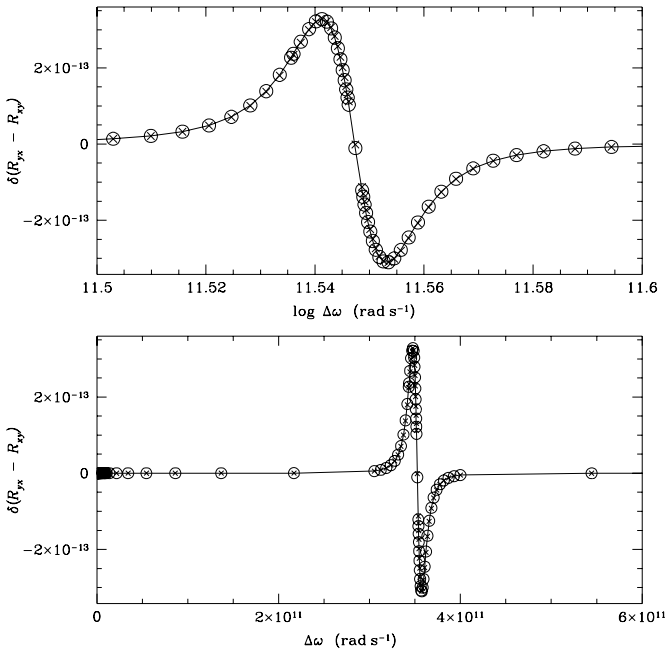

Fig. 15. Same as Fig. 10 for the function $\delta(R_{yx} - R_{xy})$. This profile is symmetrical about the line centre

of the Lorentz field with the Doppler shift, this anisotropy does not disappear after average over the velocities of the hydrogen atoms. This effect increases the complexity of the velocity average procedure. In the case where the Lorentz field effect can be treated through the perturbation theory, the average is greatly simplified. We have illustrated this for the line Lyα, using an approximate description of the Stark broadening by the plasma. This application has been carried out using a scalar damping operator, to simplify the discussion. A more realistic computation should take the tensorial nature of γ into account. We checked that, in that case, the line shapes may still be expanded in u^2, hence the conclusions reached here are not affected by the simple model that has been adopted.

The complete profile computation, including the average over the velocity of the radiating hydrogen atoms, will be presented in a next paper. For large electronic densities, obeying Eq. (44) for the Lyα line, this average will be performed using the method presented in Sect. 2, which introduces new universal functions, g_0 and g_{cross}. It depends on the angle θ between the magnetic field and the light propagation vector. For lower densities, the average over the velocity is more complicated, and it must be carried out using Eq. (19). We shall also, in the future, consider other hydrogen lines besides Lyα, in particular the first transitions of the Balmer series, which are of great interest for astrophysical applications.

Acknowledgements. We thank V. Bommier for useful discussions.

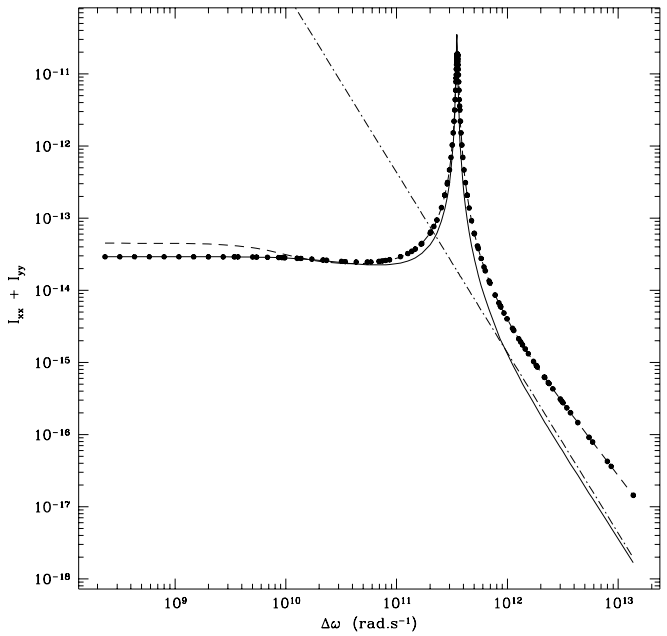

Fig. 16. Line shapes $I_{xx} + I_{yy}$ for the same plasma conditions (temperature, density, magnetic field) as in Fig. 4, calculated with different choices of the damping rate γ: *solid curve*: frequency dependent operator $\gamma(\Delta\omega)$; *dots*: frequency independent operator $\gamma(0)$; *dashed curve*: frequency independent scalar $\gamma(0)$, as used in the text and in the other illustrations. The Holtsmark static wing proportional to $|\Delta\omega|^{-5/2}$ is also plotted (*dash-dotted curve*)

Appendix A: Liouville space

$|a\alpha\gg$ denotes the Liouville state defined in terms of Hilbert states $|a>$, $|\alpha>$ as

$$|a\alpha\gg = |a><\alpha| \,. \tag{A1}$$

The generalized evolution operator $\mathcal{T}(t,0)$ is defined in terms of the Hilbert evolution operators $T(t,0)$ as

$$\ll a\alpha|\mathcal{T}|b\beta\gg = <a|T|b><\alpha|T|\beta>^* \,. \tag{A2}$$

The Hilbert evolution operator $T(t,0)$ is solution of the Schrödinger equation,

$$i\hbar\,\frac{dT}{dt} = H\,T \,, \tag{A3}$$

with $T(0,0) = 1$ (1 is the unit tensor). The generalized evolution operator $\mathcal{T}(t,0)$ is solution of

$$i\hbar\,\frac{d\mathcal{T}}{dt} = L\,\mathcal{T} \,, \tag{A4}$$

with $\ll a\alpha|L|b\beta\gg = H_{ab}\,\delta_{\alpha\beta} - H_{\alpha\beta}\,\delta_{ab}$.

Appendix B: Expressions of the dipole components

The expressions of the dipole components D_x, D_y, D_z in terms of the projections d^1_q (with $q = -1, 0, +1$) of the irreducible tensor d^1 (Edmons 1974) are

$$\begin{aligned} D_x &= \frac{-1}{\sqrt{2}}\,(d^1_1 - d^1_{-1}) \,, \\ D_y &= \frac{i}{\sqrt{2}}\,(d^1_1 + d^1_{-1}) \,, \\ D_z &= d^1_0 \,. \end{aligned} \tag{B1}$$

This decomposition is suitable to obtain the matrix elements $<a|D_k|\alpha>$ between the hydrogen states a and α. The wave functions ψ_{nlm} of the hydrogen bound electron (spherical coordinates r_e, θ_e, ϕ_e) are defined in terms of the spherical harmonics Y_{lm} (Edmons 1974; Bethe & Salpeter 1957) as

$$\psi_{nlm}(\theta_e, \phi_e) = Y_{lm}(\theta_e, \phi_e)\, R_{nl}(r_e) \,. \tag{B2}$$

Dipolar transitions are allowed between states nlm and $n'l'm'$ with $|l - l'| = 1$. One has, for example,

$$\begin{aligned} <n,l,m|d^1_q|n',l+1,m'> &= \delta_{m',m-q}\,(-1)^{l-m} \\ &\times \begin{pmatrix} l & 1 & l+1 \\ -m & q & m' \end{pmatrix} <n,l||d^1||n',l+1> \,, \end{aligned} \tag{B3}$$

with

$$\begin{aligned} <n,l||d^1||n',l+1> &= -e\,\sqrt{l+1} \\ &\times \int_0^\infty dr\, R^*_{nl}(r)\, r^3\, R_{n',l+1}(r) \\ &= -<n',l+1||d^1||n,l> \,. \end{aligned} \tag{B4}$$

Thus, one obtains

$$\begin{aligned} D_x\,D_x + D_y\,D_y &= -(d^1_1\,d^1_{-1} + d^1_{-1}\,d^1_1) \,, \\ D_x\,D_x - D_y\,D_y &= d^1_1\,d^1_1 + d^1_{-1}\,d^1_{-1} \,, \\ D_x\,D_y - D_y\,D_x &= i\,(d^1_{-1}\,d^1_1 - d^1_1\,d^1_{-1}) \,, \\ D_x\,D_y + D_y\,D_x &= -i\,(d^1_1\,d^1_1 - d^1_{-1}\,d^1_{-1}) \,, \\ D_x\,D_z + D_z\,D_x &= \frac{1}{\sqrt{2}}\,(d^1_{-1}\,d^1_0 + d^1_0\,d^1_{-1} - d^1_1\,d^1_0 - d^1_0\,d^1_1) \,, \\ D_x\,D_z - D_z\,D_x &= \frac{1}{\sqrt{2}}\,(d^1_{-1}\,d^1_0 + d^1_0\,d^1_1 - d^1_1\,d^1_0 - d^1_0\,d^1_{-1}) \,, \\ D_y\,D_z + D_z\,D_y &= \frac{i}{\sqrt{2}}\,(d^1_1\,d^1_0 + d^1_0\,d^1_1 + d^1_{-1}\,d^1_0 + d^1_0\,d^1_{-1}) \,, \\ D_z\,D_z &= d^1_0\,d^1_0 \,. \end{aligned} \tag{B5}$$

Appendix C: various simplifications

C.1. Simplification of b *in the case of axial symmetry*

This simplification is illustrated for $D_x\,D_x - D_y\,D_y$. Developing it in terms of irreducible components, one gets

$$\begin{aligned} D_x\,D_x &- D_y\,D_y \\ &= \sum_{a\alpha,b\beta} (d^1_{1,a\alpha}\,d^{1*}_{1,\beta b} - d^1_{-1,a\alpha}\,d^{1*}_{-1,\beta b})\,\mathcal{T}_{a\alpha,b\beta} \,. \end{aligned} \tag{C1}$$

The selection rules on the magnetic quantum numbers m_a, m_α, m_b, and m_β are obtained using the decomposition of d^1_{ij} in

terms of the $3j$ coefficients (Appendix B). The term $d^1_{1,a\alpha}\, d^1_{1,b\beta}$ is found to be proportional to

$$\begin{pmatrix} l_a & 1 & l_\alpha \\ -m_a & 1 & m_\alpha \end{pmatrix} \begin{pmatrix} l_\beta & 1 & l_b \\ -m_\beta & 1 & m_b \end{pmatrix}, \tag{C2}$$

hence it is nonzero only provided that $m_a - m_\alpha = 1 = -(m_b - m_\beta)$.

In the case of axial symmetry $\mathcal{T}_{a\alpha,b\beta}$ is equal to zero if $m_a - m_\alpha$ differs from $m_b - m_\beta$. Thus the term in $D_x\, D_x - D_y\, D_y$ of Eq. (11) is equal to 0.

C.2. Simplification of Eq. (11)

As an illustration, let us show that $D_x\, D_y + D_y\, D_x$ cancels out. The generalization to the other terms having the same property is straightforward.

$$\begin{aligned} & D_x\, D_y + D_y\, D_x \\ & = -i \sum_{a\alpha,b\beta} (d^1_{1,a\alpha}\, d^{1*}_{1,\beta b} - d^1_{-1,a\alpha}\, d^{1*}_{-1,\beta b})\, \mathcal{T}_{a\alpha,b\beta} \\ & = -i \sum d^1_{1,a\alpha}\, d^{1*}_{1,\beta b}\, \mathcal{T}_{a\alpha,b\beta} + i \sum d^{1*}_{1,\alpha,a}\, d^1_{1,b\beta}\, \mathcal{T}_{a\alpha,b\beta} \\ & = -i \sum d^1_{1,a\alpha}\, d^{1*}_{1,\beta b}\, \mathcal{T}_{a\alpha,b\beta} + i \sum d^{1*}_{1,\alpha a}\, d^1_{1,b\beta}\, \mathcal{T}_{b\beta,a\alpha} \\ & = 0\,. \end{aligned} \tag{C3}$$

C.3. Frequency integration of $\mathsf{b}_{\mathsf{cross}}$

The integral over the frequency of the Liouville time evolution operator $\mathcal{T}(t,0)$ is equal to this operator at time zero, $\mathcal{T}(0,0)$. It is equal to the unit operator in the Liouville space. Thus

$$\begin{aligned} & \int (I_{xx} - I_{yy})\, d\omega \\ & \quad = \sum_{a\alpha,b\beta} (d^1_{1,a\alpha}\, d^{1*}_{1,\beta b}\, \delta_{a\alpha}\, \delta_{b\beta} - d^1_{-1,a\alpha}\, d^{1*}_{-1,\beta b}\, \delta_{a\alpha}\, \delta_{b\beta}) \\ & \quad = 0\,. \end{aligned} \tag{C4}$$

Appendix D: velocity average for the case of small Lorentz effect

Let $\mathsf{c}_{0(\mathsf{cross}),\perp,\theta}$ be the average of the contribution $u_\perp^2\, \mathsf{b}^{(2)}$ over ϕ and $u_\perp$. Then, one has

$$\begin{aligned} \mathsf{b}_{0(\mathsf{cross})}(\tilde\omega,\theta) &= g_{\mathrm{Dopp}} * \mathsf{b}_{0(\mathsf{cross}),\perp,\theta}(\tilde\omega) \\ &+ g_{\parallel,\theta} * \mathsf{c}_{0(\mathsf{cross}),\perp,\theta}(\tilde\omega)\,. \end{aligned} \tag{D1}$$

The function $\mathsf{c}_{0(\mathsf{cross}),\perp,\theta}$ is given by

$$\mathsf{c}_{0(\mathsf{cross}),\perp,\theta}(\tilde\omega) = (g_{0(cross),\perp,\theta} * \mathsf{b}^{(2)}_{0(\mathsf{cross})})(\tilde\omega)\,, \tag{D2}$$

where the two functions $g_{0(cross),\perp,\theta}$, are defined as

$$\begin{aligned} g_{0,\perp,\theta}(\tilde\omega) &= \frac{1}{\pi\, \sin^2\theta} \int_0^\infty du_\perp\, \exp\left(-\frac{u_\perp^2}{\sin^2\theta}\right) u_\perp \\ &\times \int_{-\pi}^{+\pi} d\phi\, \delta(\tilde\omega - u_\perp\, \sin\phi)\,, \end{aligned}$$

$$\begin{aligned} g_{cross,\perp,\theta}(\tilde\omega) &= \frac{1}{\pi\, \sin^2\theta} \int_0^\infty du_\perp\, \exp\left(-\frac{u_\perp^2}{\sin^2\theta}\right) u_\perp \\ &\times \int_{-\pi}^{+\pi} d\phi\, \cos 2\phi\, \delta(\tilde\omega - u_\perp\, \sin\phi)\,. \end{aligned} \tag{D3}$$

They can be simplified as

$$\begin{aligned} g_{0,\perp,\theta}(\tilde\omega) &= \frac{\sin\theta}{\sqrt{\pi}}\, \exp\left(-\frac{\tilde\omega^2}{\sin^2\theta}\right) \left(\frac{\tilde\omega^2}{\sin^2\theta} + \frac{1}{2}\right), \\ g_{cross,\perp,\theta}(\tilde\omega) &= \frac{\sin\theta}{\sqrt{\pi}}\, \exp\left(-\frac{\tilde\omega^2}{\sin^2\theta}\right) \left(-\frac{\tilde\omega^2}{\sin^2\theta} + \frac{1}{2}\right). \end{aligned} \tag{D4}$$

One introduces

$$g_{0(cross)} = g_{\parallel,\theta} * g_{0(cross),\perp,\theta} \tag{D5}$$

The expressions (26) and (27) for those functions are obtained by using the properties of the Fourier transform of the convolution product.

References

Bethe H.A., Salpeter E.E, 1957, Quantum Mechanics of one- and two-electron atoms, Springer, Berlin

Brissaud A., Frisch U., 1971, JQSRT 11, 1167

Derevianko A., Oks E., 1997, Rev. Sci. Instrum. 68, 998

Edmons A.R., 1974, Angular Momentum in Quantum Mechanics, Princeton University Press, Princeton

Kelleher D.E., Wiese M.L., 1973, Phys. Rev. Lett. 31, 1431

Landstreet J.D., 1982, ApJ 258, 639

Landstreet J.D., Borra E.F., Angel J.R.P., Illing R.M.E., 1975, ApJ 201, 624

Mathys G., 1983, A&A 125, 13

Mathys G., 1984a, A&A 139, 196

Mathys G., 1984b, A&A 141, 248

Mathys G., 1985, Hydrogen line formation in dense plasmas in the presence of a magnetic field. In: Progress in Stellar Spectral Line Formation Theory, J.E. Beckman, L. Crivellari (eds.). Reidel, Dordrecht, p. 381

Mathys G., 1990, JQSRT 44, 143

Nguyen-Hoe, Drawin H.-W., 1973, Z. Naturforsch., A 28, 789

Nguyen-Hoe, Drawin H.-W., Herman L., 1966, Z. Naturforsch., A 21, 1515

Nguyen-Hoe, Drawin H.-W., Herman L., 1967 JQSRT 7, 429

Nguyen-Hoe, Grumberg J., Caby M., Leboucher E., Coulaud G., 1981, Phys. Rev. A 24, 438

North P., Kroll R., 1989, A&AS 78, 325

Stehlé C., 1994, A&AS 104, 509

Stehlé C., Mazure A., Nollez G., Feautrier N., 1983, A&A 127, 263

Vidal C.R., Cooper J., Smith E.W., 1970, JQSRT 10, 1011

Voslamber D., 1995. In: Spectral Line Shapes, Vol. 8, A.D. May, J.R. Drummond, E. Oks (eds.). AIP Conf. Proc. 328, New York, p. 3